Biochimica et Biophysica Acta, 553 (1979) 365—377

BBA 78376

NANOSECOND FLUORESCENCE ANISOTROPY DECAYS OF 1,6-DIPHENYL-1,3,5-HEXATRIENE IN MEMBRANES *

KNUT HILDENBRAND and CLAUDE NICOLAU

Institut für Strahlenchemie im Max-Planck-Institut für Kohlenforschung, Stiftstr. 34-36, D-4330 Mülheim a.d. Ruhr (F.R.G.)

(Received November 1st, 1978)

Key words: Fluorescence polarization; Liposome; 1,6-Diphenyl-1,3,5-hexatriene

Summary

Nanosecond decays of the fluorescence anisotropy, r, were studied for the emission of 1,6-diphenyl-1,3,5-hexatriene (DPH) embedded in a series of mixed multilamellar liposomes containing egg yolk phosphatidylcholine, phosphatidylethanolamine and cholesterol in varying molar ratios, as well as in membranes of intact cells and in virus envelopes.

The relative contributions of the fast and the infinitely slow decaying component to the steady-state value, $\bar{r}$, of the fluorescence anisotropy were very similar for artifical and biological membranes.

Angles, θ, of the cone, by which the motion of the fluorescent molecule is limited, were calculated from the intensity of the infinitely slow decaying anisotropy component and compared with steady-state fluorescence anisotropies and with 'microviscosities', $\langle\eta\rangle$. An increase in $\langle\eta\rangle$ from 1.5 to 5.2 P in our systems was accompanied by a decrease in θ from 49° to 30° while the decrease in the mean motional relaxation times, ϕ_f, of the label molecule was not more than 1 ns and due mainly to changes in the potential, by which the diffusion of DPH in the membrane is restricted. From these observations we conclude that differences in the steady-state fluorescence anisotropy and in 'microviscosities' of cholesterol-containing membranes ($\bar{r} > 0.15$) represent changes in the degree of static orientational constraint rather than changes in diffusion rates of the label.

---

* Dedicated to Prof. O.E. Polansky on the occasion of his 60th birthday.

Abbreviations: DPH, all *trans*-1,6-diphenyl-1,3,5-hexatriene; DMPC, dimyristoylphosphatidylcholine; DPPC, Dipalmitoylphosphatidylcholine; D_{17}, Schmidt-Ruppin induced tumors in STU-mouse fibroblasts; BHK 21, baby hamster kidney cells; LM-fibroblasts, leukaemic mouse fibroblasts; N-Egg, Avian strain of influenza virus grown in the allantoic cavity of eggs; NDV-MDBK, Newcastle disease virus strain Italien grown in MDBK cells.

Introduction

The application of single photon counting techniques, developed for long-time data acquisition and of numerical multiexponential deconvolution techniques [1—5], made possible a complete analysis of the nanosecond fluorescence anisotropy decays of all *trans*-1,6-diphenyl-1,3,5-hexatriene (DPH) in vesicles of dimyristoylphosphatidylcholine (DMPC) [1], egg yolk phosphatidylcholine [2], dipalmitoylphosphatidylcholine (DPPC) [3], in mixed liposomes of DPPC and cholesterol [6], in intact mouse leukaemic cells [7] and in human erythrocytes [8]. The main advantage of these time-resolved studies over the conventional steady-state method [9,10] is that they give a much more detailed description of the DPH motion in the membrane interior. The interpretation in terms of a 'wobbling-in-cone' model leads to parameters of orientational constraint ('cone angles') and to 'wobbling diffusion constants' [11] while the interpretation of the steady-state data in terms of 'mean correlation times' [12,13] or 'microviscosities', $\langle\eta\rangle$, [9,10] uses a physical model which is, strictly speaking, applicable to anisotropic label motions only under specific conditions (which are certainly not met in membranes [2]) and which does not take into account a restriction of label diffusion by a potential. Therefore it is not sure at all that the steady-state method gives a correct description of membrane 'fluidity'.

In our investigations we used the nanosecond technique in order to determine the dynamic and static properties of DPH in (a) a series of mixed multilamellar liposomes containing the main phospholipids of fibroblasts (i.e., phosphatidylcholine, phosphatidylethanolamine) and cholesterol in varying molar ratios and (b) membranes of intact cells and virus envelopes. This procedure offers the possibility to compare changes in steady-state and nanosecond time-resolved polarization data of DPH as a function of the varying chemical composition of the membrane systems and thus should lead to information concerning the reliability of steady-state fluorescence parameters for the description of membrane lipid dynamics.

Materials and Mehods

Systems

Model membranes. Two different systems of onion-like, multilamellar liposomes containing the main phospholipids present in fibroblast membranes (i.e. phosphatidylcholine and phosphatidylethanolamine) with varying cholesterol contents were prepared: system A: egg yolk phosphatidylcholine/cholesterol (cholesterol : phospholipid molar ratio varying from 0.2 to 1); system B: egg yolk phosphatidylcholine/phosphatidylethanolamine/cholesterol (cholesterol : phospholipid molar ratio varying from 0.33 to 1). The compositions of the samples can be seen in Tables I and II. System C: Biological membranes (see Table III).

Cells. The D_{17}, BHK 21, LM-fibroblast and HeLa cells were grown to confluence in Eagle's minimal medium with 10% new-born calf serum, harvested by mild trypsinization (0.025% trypsin, 2 min at 37° C) washed with cold phosphate-buffered saline and then resuspended in phosphate-buffered saline.

Viruses. The Newcastle disease Virus (NDV) strain Italien was grown in MDBK cells [14]. The avian strain N of influenza virus (A/Chick/Germany/49 (Hav2Neq 1)) was grown in the allantoic cavity of embryonated eggs. Virus titers have been determined by hemagglutinin and plaque assays. The viruses were purified from cell culture medium or allantoic fluid by the procedures of Klenk et al. [15].

Chemicals

Egg yolk phosphatidylcholine and phosphatidylethanolamine from egg yolk were purchased from Lipid Products, U.K. (Grade I, chromatographically pure). Cholesterol was obtained from Sigma Chemicals and DPH puriss. from Aldrich, Europe. All of these compounds were used without further purification.

Preparation of the samples

Large, multilamellar liposomes were prepared by the method of Bangham et al. [16] and Lentz et al. [17]. Mixtures of stock solutions of the lipids in $CH_3OH/CHCl_3$ were evaporated under dry N_2 to dryness. The lipids were suspended in aqueous phase containing 50 mM KCl and 15% (w/w) sucrose (ultra pure, Schwartz Mann). To a 4.5 ml portion of the suspensions (approx. 0.5 mM in lipids) 1 μl of 2 mM DPH in tetrahydrofuran was added with rapid agitation and gently swirled for 2 h before measurement.

Cells and viruses. $1 \cdot 10^6$ cells/ml or 10^{11} viruses/ml were labelled under the conditions of [9]. A tetrahydrofuran solution of $2 \cdot 10^{-3}$ M DPH was diluted 1000 fold by injection in phosphate-buffered saline, pH 7.4, with vigorous shaking. The DPH solution was stirred for 15 min at 25° C and added to the cell or virus suspension. Cells were then sedimented by centrifugation at $1200 \times g$ for 10 min viruses at $100\,000 \times g$ for 1 h and resuspended in sucrose/KCl (15%, w/w).

Fluorescence measurements

Steady-state measurements of polarization degrees. Fluorescence polarization degrees

$$\bar{p} = \frac{i_{\parallel} - i_{\perp}}{i_{\parallel} + i_{\perp}} \tag{1a}$$

were obtained with a fluoropolarimeter Elscint MV-1 at 25° C (instrumental details are described in [18]). $i_{\parallel}$ and $i_{\perp}$ are the fluorescence intensities detected through polarizers oriented in parallel ($\parallel$) and perpendicular ($\perp$) positions relative to the direction of the polarization of the excitation beam.

Fluorescence anisotropies

$$\bar{r} = \frac{i_{\parallel} - i_{\perp}}{i_{\parallel} + 2i_{\perp}} \tag{1b}$$

were calculated from $\bar{p}$ by

$$\bar{r} = \frac{2\bar{p}}{3 - \bar{p}} \tag{2}$$

In order to reduce artifacts due to depolarization of excitation and emission beams by light scattering [19,20] the samples were diluted to an absorbance

of approx. 0.15 at the non-absorbing wavelength λ = 450 nm in 10-mm quartz cells for the steady-state as well as for the nanosecond measurements.

Fluorescence lifetimes were obtained at 25° C with a single-photon instrument equipped with a gated air-filled flash lamp. The excitation light (357 nm) and emission light (430 nm) passed through interference filters with band width of 20 nm. In order to avoid an interference of the slow decay of fluorescence anisotropy with the fluorescence decay characteristics polarizers were used in the excitation and emission paths rotated at 0° and 54° 44 min from the vertical, respectively. Interference of time-dependent polarization of the emitted light with the fluorescence decays was avoided by the use of polarizers in the excitation and emission paths rotated at 0° and 54° 44 min from the vertical, respectively. The data were collected on a 6220 Ortec multichannel analyzer with 1 K data memory and transferred to a PDP 10 computer for further processing.

A single exponential decay law was used for deconvolution of the experimental fluorescence decay d(t). By a non-linear weighted least-squares fit (see, for example [3]) of

$$f(t) = ae^{-t/\langle\tau\rangle} \tag{3a}$$

to the integral

$$d(t) = \int_0^t f(t - t')g(t')dt' \tag{3b}$$

a time constant, $\langle\tau\rangle$, for the emission properties of DPH was obtained which has to be considered as a mean value of different decay times in the case of non-exponential decay behaviour as this has been described for DPH in some cases [1,2] and which may be present in our systems, too. g(t') in Eqn. 3b is the excitation function obtained with a sample of unlabelled egg yolk phosphatidylcholine vesicles in H_2O.

As $\langle\tau\rangle$ was used only for determination of 'microvisicosities', a multiexponential deconvolution is not necessary.

Nanosecond anisotropy decays. To this purpose the single-photon instrument was equipped with Glan-Thompson polarizers. The polarizer in the emission path was changed from parallel to perpendicular position relative to the direction of the polarization of the excitation beam every 30 s and the fluorescence intensity decays $i_\parallel(t)$ and $i_\perp(t)$ were stored in different memory regions of the multichannel analyzer in 256 channels. For a typical measurement about 10^6 counts were accumulated for $i_\parallel(t)$ in about 1 h. The samples were gently swirled every 10 min to prevent sedimentation of the material. The anisotropy decays were calculated according to [1—3]:

$$r(t) = \frac{F \cdot i_\parallel(t) - i_\perp(t)}{F \cdot i_\parallel(t) + 2i_\perp(t)} \tag{4}$$

The factor

$$F = \frac{1 + 2\bar{r}}{1 - \bar{r}} \cdot \frac{I_\perp}{I_\parallel} \tag{5}$$

allows for correction of fluctuations in the excitation intensity during the accumulation in the nanosecond experiment [1—3] and for possible slight anisotropic sensitivity of the detection system as to the direction of polarized light. $I_{\parallel}$ and $I_{\perp}$ are the integrated intensities in the nanosecond experiment with parallel ($\parallel$) and perpendicular ($\perp$) position of the polarizer in the emission path relative to the polarization plane of the excitation light. A slight distortion of the anisotropy decays by this procedure may occur by artifacts due to scattering depolarization and birefringence, resulting in wrong values of r_0, mainly [2]. The values of F in our measurements varied from approx. 098 to 1.04 without any systematic dependence on r. Test measurements with unlabelled liposomes showed that the contribution of scattered excitation light to the $r(t)$ functions was less than 1% even in the maximum of the scattering signal and could be neglected under our conditions.

The anisotropy decays in all our measurements consisted of a fast decay reaching a plateau about 10—20 ns after begin of the excitation flash which agrees with the results of other investigations [1—8]. The height of the plateau, r_∞, could be determined by a least-squares calculation from approx. 50 points of the $r(t)$ curve with a standard deviation of 0.005 for samples with steady-state fluorescence anisotropy values $\bar{r} > 0.15$. For samples with $\bar{r} < 0.15$, the deviations for the r_∞ values were larger because of the lower signal-to-noise ratio of the $r(t)$ values (see Fig. 1).

Interpretation of measurements

Steady-state fluorescence anisotropies. By application of the Perrin formalism for rotational depolarization of a fluorophore [21] the steady-state fluorescence anisotropy, $\bar{r}$, of DPH in membrane systems can be correlated with the 'microviscosity' $\langle\bar{\eta}\rangle$ of the interior of the bilayer by the following equation [9,10]:

$$\left(\frac{r_0}{\bar{r}} - 1\right) = C_r \frac{T\langle\tau\rangle}{\langle\bar{\eta}\rangle} \tag{6}$$

where T is the absolute temperature and r_0 the limiting fluorescence anisotropy for rigidly embedded DPH molecules, r_0 has been determined by low temperature measurements in propylene glycol ($r_0 = 0.362$) [10]. C_r is a parameter which depends on the effective molar rotational volume of the fluorescent molecule and can be evaluated for DPH in organic solvents from a Perrin plot [22]. Under these conditions, changes in the anisotropy of the label rotation are represented by changes in C_r and those in average diffusion rates by changes in 'microviscosities'.

As C_r cannot be obtained for lipid bilayers by a direct measurement it is necessary to refer to a system which is supposed to have similar properties. Shinitzky and Inbar [9] suggested to use a value of $C_r = 8.6 \pm 0.4 \cdot 10^5$ P · degree^{-1} · s^{-1} from a Perrin plot for DPH in 'American White Oil U.S.P. 35' in order to determine membrane 'microviscosities'.

By this procedure it is not possible to distinguish between changes in the anisotropy of label rotation and in the absolute value of the average diffusion constant. Moreover, differences in static constraints of DPH in the lipid bilayers

might also contribute to the value of the complex steady-state parameters $\bar{r}$ and $\langle\bar{\eta}\rangle$ but are not taken into account in the 'microviscosity' concept.

The decay of the total fluorescence inensity ($i_{\parallel} + 2i_{\perp}$) of DPH in lipid bilayers could not be described by a single exponential function in all cases [1,2,7]. The reasons for this behaviour are not yet clear. Microheterogeneity of sites for the probe in the bilayer, a reversible excited-state reaction and solvent-dependent excited-state isomerizations are considered as possible origins for this behaviour [1,2,23,24]. No matter what the exact interpretation may be, the evaluation of steady-state fluorescence polarization data in terms of 'microviscosities' by comparison with a reference medium is complicated by this fact. As we did not use correction procedures for the instrument response function and numerical multiexponential deconvolution techniques [1—5,7] we are not able to draw any conclusions about the emission kinetics of DPH in our samples and we use an average value of $\langle\tau\rangle$ for the time constant of the emission decay in Eqn. 6 to account for the possibility of complex decay behaviour.

Nanosecond anisotropy decays of DPH in cholesterol-containing membranes. Fluorescence anisotropy decays of DPH reaching a plateau on the nanosecond time scale can be characterized by:

$$r(t) = (r_0 - r_\infty) \exp^{-t/\phi_f} + r_\infty \tag{7}$$

The interpretation of Eqn. 7 may be based upon a model which assumes anisotropic orientational distribution of DPH at equilibrium state; r_∞/r_0 represents the degree of mean orientation of the label and ϕ_f the relaxation time into the anisotropic equilibrium distribution [3,11]. These properties are very similar to those assumed for spin labels in membranes [25,26]. The excited DPH would undergo a wobbling diffusion within a cone around the normal of the membrane with the cone angle $\theta(0° \leqslant \theta \leqslant 90°)$. The 'wobbling diffusion constant', D_w, is supposed to be constant throughout the cone. It may be calculated from the time course of the fast decaying anisotropy component:

$$\frac{r(t)}{r_0} = \sum_{i=1}^{\infty} A_i \exp \frac{-D_w \cdot t}{\sigma_i} \tag{8}$$

where A_i and σ_i are constants which depend on the angle of the cone only. (Values for A_i and σ_i can be obtained from plots in [11].)

θ can be calculated from

$$\frac{r_\infty}{r_0} = [\tfrac{1}{2} \cos\theta(1 + \cos\theta)]^2 \tag{9}$$

The motional relaxation time, ϕ_f, may be expressed as the average of relaxation times according to

$$\phi_f \simeq \langle\phi_f\rangle = \frac{1}{D_w} \frac{\sum_i A_i\sigma_i}{\sum_i A_i} \approx \frac{\langle\sigma\rangle}{D_w} \tag{10}$$

Thus, ϕ_f depends not only on the 'wobbling diffusion constant' but also on the 'cone angle' and for this reason does not represent the 'diffusion rate' of the label.

Correlation of steady-state and time-resolved fluorescence anisotropy of DPH embedded in membranes. By integration over an infinite number of excitation flashes the value of the steady-state fluorescence anisotropy, $\bar{r}$, can be calculated from the characteristics of the corresponding fluorescence anisotropy decay [27] by

$$\bar{r} = \frac{\int_0^\infty [i_\parallel(t) - i_\perp(t)]\mathrm{d}t}{\int_0^\infty [i_\parallel(t) + 2i_\perp(t)]\mathrm{d}t} = \int_0^\infty r(t)\mathrm{d}t \tag{11}$$

With $r(t)$ from Eqn. 7 we obtain, in analogy to the derivation of Perrin's equation [27]

$$\bar{r} = \frac{r_0 - r_\infty}{1 + \frac{\langle\tau\rangle}{\phi_f}} + r_\infty = \bar{r}_f + r_\infty \tag{12}$$

which means that the steady-state value of $\bar{r}$ for DPH, embedded in membranes, contains contributions from the fast and the infinitely slow decaying components.

Results and Discussion

An important application of the DPH fluorescence probe originates from the investigation of 'mobility' differences in the hydrophobic part of lipid membranes with regard to biological functions (e.g. [13]). However, in view of the results of nanosecond studies [1—3,6—8,11] the characterization of membranes by 'microviscosities' is complicated due to the restricted rotational diffusion of the label molecule in a potential and due to the complexity of its emission kinetics.

Therefore, a comparison of steady-state and time-resolved fluorescence depolarization measurements of DPH in a variety of membranes seems to be advisable.

For this purpose we calculated from the $r(t)$ curves (e.g. Fig. 1) the height of the plateau, r_∞, reached for the stationary orientational distribution of emission dipoles of DPH at about 10—20 ns after the end of photoselection.

The difference between $\bar{r}$ and r_∞ gives the contribution of the fast decaying fluorescence anisotropy component, r_f, to the steady-state anisotropy $\bar{r}$ (see Eqn. 12). A plot of r_f and r_∞ vs. $\bar{r}$ illustrates the relative contributions of the two terms of the nanosecond anisotropy decays to $\bar{r}$. From Fig. 2 we see that an increase in r is caused by increasing r_∞ values while r_f decreases. The ratio of r_f/r_∞ is quite similar for artificial and biological membranes with identical $\bar{r}$ values. It is interesting to note that even for the 'fluid' membranes with cholesterol/phospholipid molar ratios of 0.2 the contribution of the infinitely

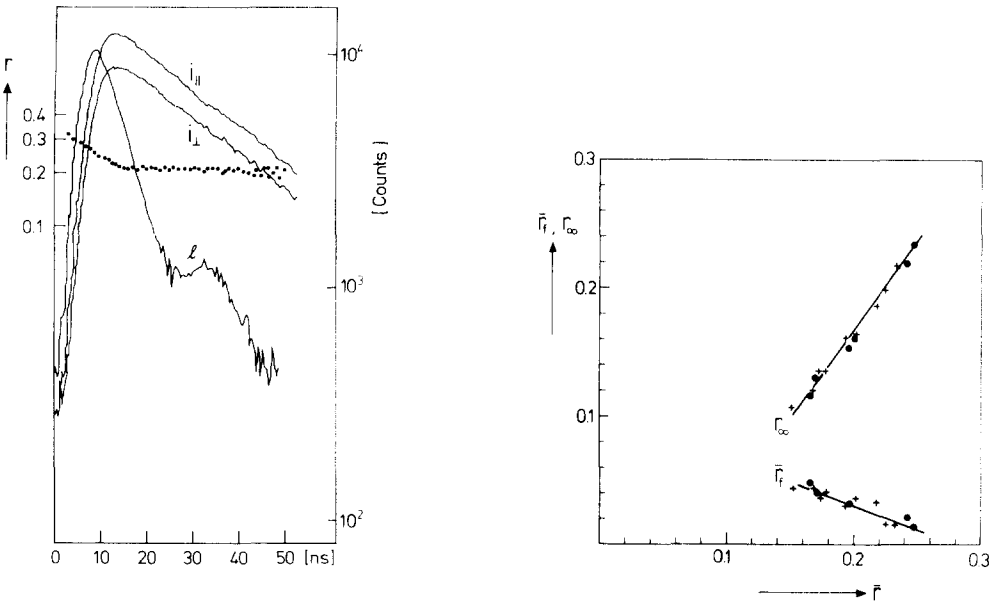

Fig. 1. Time dependence of the fluorescence anisotropy r (· · · · · ·) of DPH embedded in the envelope of influenza virus grown in the alantoic cavity of embryonated eggs (N-Egg). $i_{\parallel}$ and $i_{\perp}$, the decays of fluorescence intensities of DPH with polarizers in parallel and perpendicular positions. l, the uncorrected instrument response function obtained with a scattering sample.

Fig. 2. Relative contributions of the fast (r_f) and the infinitely slow decaying component (r_∞) of $r(t)$ to the steady-state value of $\bar{r}$. +, system A (egg yolk phosphatidylcholine/cholesterol in varying molar ratios); •, system C (biological membranes).

slow decaying component to $\bar{r}$ is about 70%, and reaches a value of approx. 90% for the 'rigid' membranes with equimolar amounts of cholesterol and phospholipids.

By application of the 'wobbling-in-cone' model for rotational diffusion of DPH in a potential [11] we calculated the cone angles for all our samples from r_∞ and r_0 (Eqn. 9).

Extrapolation of the $r(t)$ curves to zero time yielded r_0 values in the range of 0.30—0.34. No systematic dependence of r_0 on the chemical composition of the membranes could be obtained within the limits of error. It is known from previous investigations [1—3,7] that r_0 values obtained by an analysis of nanosecond anisotropy decays of DPH in membranes are not very reliable due to the low signal-to-noise ratio of the $r(t)$ curve for $t \to 0$ and to artifacts such as light scattering and birefringence (see Materials and Methods). Therefore, for the calculation of cone angles we used the same value of the limit anisotropy (r_0 = 0.362 [10]) as for the evaluation of 'microviscosities' (Eqns. 9 and 6, respectively).

For a comparison of steady-state fluorescence anisotropy with the mean static orientation of DPH relative to the normal of the bilayer we plotted θ vs. the corresponding values of $\bar{r}$ and obtained very similar correlations for the multilamellar liposomes and for the biological systems (Fig. 3). The significant dependence of $\bar{r}$ on θ is reminiscent of an observation reported for $\bar{r}$ of DPH in

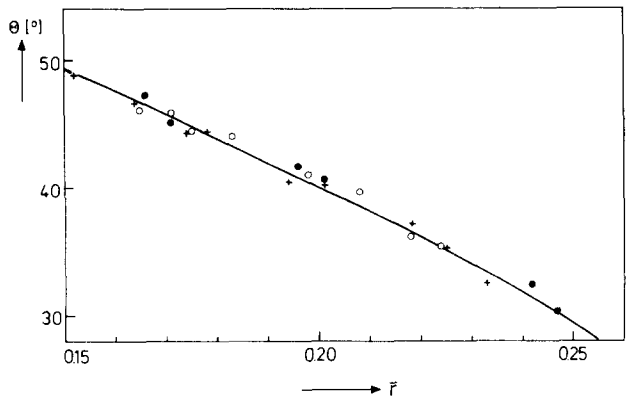

Fig. 3. Plot of cone angles vs. $\bar{r}$ for +, system A (egg yolk phosphatidylcholine/cholesterol with varying molar ratios); ○, system B (egg yolk phosphatidylcholine/phosphatidylethanolamine/cholesterol with varying molar ratios); ●, system C (biological membranes).

DPPC vesicles undergoing a thermotropic phase transition at 42°C. In this system the sigmoidal shape of the steady-state fluorescence anisotropy as function of the temperature was accompanied by a dramatic change in cone angles [3]. In view of the correlation of $\bar{r}$ and θ and in view of the fact that the mean lifetimes $\langle\tau\rangle$ of DPH in our systems are dependent on the motional state of the surrounding matrix (see for example [3,10]) it is not surprising that changes in cone angles are accompanied by large changes in 'microviscosities'.

So, for example, for the biological systems an interval in θ for DPH from approx. 46° in D_{17} cells to approx. 35° in NDV corresponds to an increase in $\langle\bar{\eta}\rangle$ from approx. 1.7 to approx. 5.2 P (see Fig. 4).

While from r_∞ we evaluated the static parameter θ, it is possible to get information about the dynamic properties of the label from the fast decaying component of the fluorescence anisotropy decays.

Because of the difficulties originating in long accumulation times and

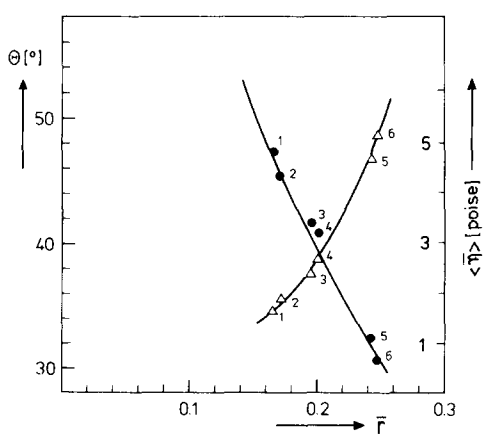

Fig. 4. Plot of cone angles, θ (●) and 'microviscosities', $\langle\eta\rangle$ (△) vs. r for system C. 1, D_{17}; 2, BHK 21; 3, LM-fibroblasts; 4, HeLa; 5, N-Egg; 6, NDV-MDBK.

TABLE III

FLUORESCENCE PARAMETERS FOR DPH IN BIOLOGICAL MEMBRANES (SYSTEM C)

Values were calculated or experimentally determined as described in Table I.

	$\bar{r}$	r_∞	$\langle\tau\rangle$ (ns)	$\bar{r}_f$	$\theta(^\circ)$	ϕ_f (ns)	$\langle\bar{\eta}\rangle$ (P)
1 $D_{1\,7}$	0.166 ± 0.005	0.117 ± 0.005	7.8 ± 0.4	0.049 ± 0.005	47.3 ± 0.8	1.9 ± 0.6	1.69 ± 0.4
2 BHK 21	0.171 ± 0.005	0.130 ± 0.005	8.4 ± 0.4	0.041 ± 0.005	45.2 ± 0.8	1.9 ± 0.6	1.92 ± 0.4
3 LM-fibroblasts	0.196 ± 0.005	0.153 ± 0.005	8.0 ± 0.4	0.043 ± 0.005	41.8 ± 0.8	2.1 ± 0.6	2.42 ± 0.4
4 HeLa	0.201 ± 0.005	0.161 ± 0.005	8.6 ± 0.4	0.050 ± 0.005	40.6 ± 0.8	2.1 ± 0.6	2.75 ± 0.4
5 N-Egg	0.242 ± 0.005	0.219 ± 0.005	9.2 ± 0.4	0.023 ± 0.005	32.5 ± 0.8	1.8 ± 0.6	4.75 ± 0.4
6 NDV-MDBK	0.247 ± 0.005	0.234 ± 0.005	9.5 ± 0.4	0.013 ± 0.005	30.3 ± 0.8	1.1 ± 0.6	5.22 ± 0.4

TABLE I

FLUORESCENCE DATA FOR DPH IN LARGE MULTILAMELLAR LIPOSOMES WITH VARYING AMOUNTS OF CHOLESTEROL (SYSTEM A)

$\bar{r}$, calculated from the experimentally determined $\bar{p}$ values using Eqn. 2; $\bar{r}_\infty$ and $\langle\tau\rangle$, experimentally determined; $\bar{r}_f$, calculated from $\bar{r}$ and r_∞ by Eqn. 12; θ calculated from r_∞ by Eqn. 9 ($r_0 = 0.362$); ϕ_f, calculated from $\bar{r}$, r_∞, and $\langle\tau\rangle$ from Eqn. 12 ($r_0 = 0.362$); $\langle\eta\rangle$, calculated from $\bar{r}$ and $\langle\tau\rangle$ by Eqn. 6 ($r_0 = 0.362$; $C_r = 8.6 \cdot 10^5$ P · degree^{-1} · s^{-1} [20]). PC, egg yolk phosphatidylcholine; chol., cholesterol.

Molar ratio PC/Chol.	$\bar{r}$	$\bar{r}_\infty$	$\langle\tau\rangle$ (ns)	$\bar{r}_f$	$\theta(^\circ)$	ϕ_f (ns)	$\langle\bar{\eta}\rangle$ (P)
1 : 0.2	0.152 ± 0.005	0.107 ± 0.005	8.6 ± 0.4	0.045 ± 0.005	48.9 ± 0.8	1.8 ± 0.6	1.59 ± 0.4
1 : 0.3	0.164 ± 0.005	0.120 ± 0.005	8.7 ± 0.4	0.044 ± 0.005	46.8 ± 0.8	1.9 ± 0.6	1.84 ± 0.4
1 : 0.4	0.174 ± 0.005	0.136 ± 0.005	8.8 ± 0.4	0.038 ± 0.005	44.4 ± 0.8	1.8 ± 0.6	2.08 ± 0.4
1 : 0.5	0.178 ± 0.005	0.136 ± 0.005	9.0 ± 0.4	0.042 ± 0.005	44.4 ± 0.8	1.7 ± 0.6	2.23 ± 0.4
1 : 0.6	0.194 ± 0.005	0.162 ± 0.005	9.2 ± 0.4	0.032 ± 0.005	40.5 ± 0.8	1.8 ± 0.6	2.72 ± 0.4
1 : 0.7	0.201 ± 0.005	0.164 ± 0.005	9.3 ± 0.4	0.037 ± 0.005	40.2 ± 0.8	2.1 ± 0.6	2.97 ± 0.4
1 : 0.8	0.218 ± 0.005	0.185 ± 0.005	9.4 ± 0.4	0.033 ± 0.005	37.2 ± 0.8	2.2 ± 0.6	3.64 ± 0.4
1 : 0.9	0.225 ± 0.005	0.199 ± 0.005	9.6 ± 0.4	0.016 ± 0.005	35.3 ± 0.8	1.0 ± 0.6	4.04 ± 0.4
1 : 1.0	0.233 ± 0.005	0.218 ± 0.005	9.7 ± 0.4	0.015 ± 0.005	32.6 ± 0.8	1.1 ± 0.6	4.49 ± 0.4

TABLE II

FLUORESCENCE DATA FOR DPH IN LARGE MULTILAMELLAR LIPOSOMES WITH VARYING AMOUNTS OF CHOLESTEROL (SYSTEM B)

Values were calculated or experimentally determined as described in Table I. PC, egg yolk phosphatidylcholine; PE, phosphatidylethanolamine; chol; cholesterol.

Molar ratio PC/Chol.	$\bar{r}$	r_∞	$\langle\tau\rangle$ (ns)	$\bar{r}_f$	$\theta(^\circ)$	ϕ_f (ns)	$\langle\bar{\eta}\rangle$ (P)
1 : 1 : 0.66	0.165 ± 0.005	0.124 ± 0.005	7.8 ± 0.4	0.041 ± 0.005	46.2 ± 0.8	1.6 ± 0.6	1.67 ± 0.4
1 : 1 : 0.83	0.171 ± 0.005	0.126 ± 0.005	8.2 ± 0.4	0.045 ± 0.005	45.9 ± 0.8	1.9 ± 0.6	1.88 ± 0.4
1 : 1 : 1.0	0.175 ± 0.005	0.134 ± 0.005	8.2 ± 0.4	0.041 ± 0.005	44.6 ± 0.8	1.8 ± 0.6	1.96 ± 0.4
1 : 1 : 1.17	0.183 ± 0.005	0.138 ± 0.005	8.5 ± 0.4	0.045 ± 0.005	44.1 ± 0.8	2.1 ± 0.6	2.22 ± 0.4
1 : 1 : 1.33	0.198 ± 0.005	0.158 ± 0.005	8.5 ± 0.4	0.040 ± 0.005	41.1 ± 0.8	2.1 ± 0.6	2.62 ± 0.4
1 : 1 : 1.5	0.208 ± 0.005	0.174 ± 0.005	8.4 ± 0.4	0.034 ± 0.005	38.9 ± 0.8	1.9 ± 0.6	2.90 ± 0.4
1 : 1 : 1.67	0.218 ± 0.005	0.192 ± 0.005	8.5 ± 0.4	0.026 ± 0.005	36.2 ± 0.8	1.5 ± 0.6	3.28 ± 0.4
1 : 1 : 2.0	0.224 ± 0.005	0.198 ± 0.005	8.7 ± 0.4	0.026 ± 0.005	35.4 ± 0.8	1.6 ± 0.6	3.62 ± 0.4

numerical multiexponential deconvolution we were not able to determine experimentally ϕ_f, the time constant for motional relaxation in the cone.

However, by a rough estimation from Eqn. 12 with the experimentally determined parameters $\bar{r}$, r_∞ and $\langle\tau\rangle$ we obtained values of approx. 1—2 ns for ϕ_f (see Tables I—III). This result is very similar to the one obtained by direct deconvolution of the nanosecond fluorescence anisotropy decays of DPH in DPPC near the thermotropic phase transition [3] (θ of approx. 30—50°, ϕ_f approx. 1.0—1.5 ns in the temperature range from approx. 37 to 40°C).

As the 'wobbling-in-cone' theory [11] predicts an increase in $\langle\sigma\rangle$ (Eqn. 10) from approx. 0.1 to approx. 0.2 for the interval of cone angles from approx. 30° to 50° we conclude that the value for the diffusion constant in the cone, D_w, is about the same in all our systems (approx. 0.08 ± 0.05 ns^{-1}) or, in other words, a decrease in mean motional relaxation time, ϕ_f, can be explained by an increase in the degree of static orientation of DPH, only.

This means that changes in steady-state fluorescence anisotropies of DPH embedded in cholesterol-containing membranes ($\bar{r} > 0.15$), mainly represent changes in the static properties of DPH. A small contribution ($r_{f/r} < 0.3$) to the value of $\bar{r}$ of DPH in those systems arises from the motional relaxation of DPH molecules. The influence of this term on $\bar{r}$ is dependent not only on ϕ_f but also on the average fluorescence lifetime $\langle\tau\rangle$ of the probe. This fact causes uncertainties in the correlation of $\bar{r}$ and θ values (Fig. 3), making the steady-state parameter less reliable for the characterization of lipid 'mobility' than results from time-resolved polarization experiments. Changes in 'microviscosities', evaluated from $\bar{r}$ by application of Eqn. 6 should be considered as semiempirical indications for a combination of changes in the degree of orientational constraint and in lifetimes of DPH in the lipid bilayers, and, in general, will not lead to wrong information about the ordering of DPH in the membrane interior. However, a comparison of membranes based on the 'microviscosity' concept should be treated with caution in view of the complex theoretical and experimental background of this parameter.

Acknowledgements

The authors thank Prof. H.D. Klenk of the Institut für Virologie at the Justus-Liebig-Universität, Giessen for the virus systems and Miss I. Hengst for excellent technical assistance.

References

1 Chen, L.A., Dale, R.E., Roth, S. and Brand, L. (1977) J. Biol. Chem. 252, 2163—2169
2 Dale, R.E., Chen, L.A. and Brand, L. (1977) J. Biol. Chem. 252, 7500—7511
3 Kawato, S., Kinosita, K., Jr. and Ikegami, A. (1977) Biochemistry 16, 2319—2324
4 Rayner, D.M., McKinnon, A.E. and Szabo, A.G. (1977) Rev. Sci. Instrum. 48, 1050—1054
5 McKinnon, A.E., Szabo, A.G. and Miller, D.R. (1977) J. Phys. Chem. 81, 1564—1570
6 Veatch, W.R. and Stryer, L. (1977) Biophys. Soc. Abstr. Biophys. J. 21, 69a
7 Sené, C., Genest, D., Obrénovitch, A., Wahl, P. and Monsigny, M. (1978) FEBS Lett. 88, 181—186
8 Glatz, P. (1978) Anal. Biochem. 87, 187—194
9 Shinitzky, M. and Inbar, M. (1974) J. Mol. Biol. 85, 603—615
10 Shinitzky, M. and Barenholz, Y. (1974) J. Biol. Chem. 249, 2652—2657
11 Kinosita, K.J., Jr., Kawato, S. and Ikegami, A. (1977) Biophys. J. 20, 289—305

12 Bashford, C.L., Morgan, C.G. and Radda, G.K. (1976) Biochim. Biophys. Acta 426, 157—172
13 Nicolau, C., Hildenbrand, K., Reimann, A., Johnson, S.M., Vaheri, A. and Friis, R. (1978) Exp. Cell. Res. 113, 63—73
14 Nagai, Y., Klenk, H.D. and Rott, R. (1976) Virology 72, 494—508
15 Klenk, H.D., Becht, H. and Rott, R. (1972) Virology 47, 579—591
16 Bangham, A.D., DeGier, J. and Greville, G.D. (1967) Chem. Phys. Lipids I, 225
17 Lentz, B.R., Barenholz, Y. and Thompson, T.E. (1976) Biochemistry 15, 4521—4528
18 Roche, A.C., Maget-Dana, R., Obrenovitch, A., Hildenbrand, K., Nicolau, C. and Monsigny, M. (1978) FEBS Lett. 93, 91—96
19 Teale, F.W.J. (1969) Photochem. Photobiol. 10, 363—374
20 Johnson, S.M. and Nicolau, C. (1977) Biochem. Biophys. Res. Commun. 76, 869—874
21 Weber, G. (1953) Adv. Protein Chem. 8, 415—459
22 Hare, F. and Lussan, C. (1977) Biochim. Biophys. Acta 467, 262—272
23 Cehelnik, E.D., Cundall, R.B., Lockwood, J.R. and Palmer, T.F. (1975) J. Phys. Chem. 79, 1369—1376
24 Mason, R. and Cehelnik, E.D. (1978) J. Photochem. 9, 219—221
25 Hubbell, W.L. and McConnell, H.M. (1969) Proc. Natl. Acad. Sci. U.S. 64, 20—27
26 Jost, P., Libertini, L.J., Hebert, V.C. and Griffith, O.H. (1971) J. Mol. Biol. 59, 77—98
27 Wahl, P. (1975) Biochemical Fluorescence Concepts (Chen, R.F. and Edelhoch, H., eds.), Vol. I, pp. 1—41, Marcel Dekker, Inc., New York